1 Momentum Theory

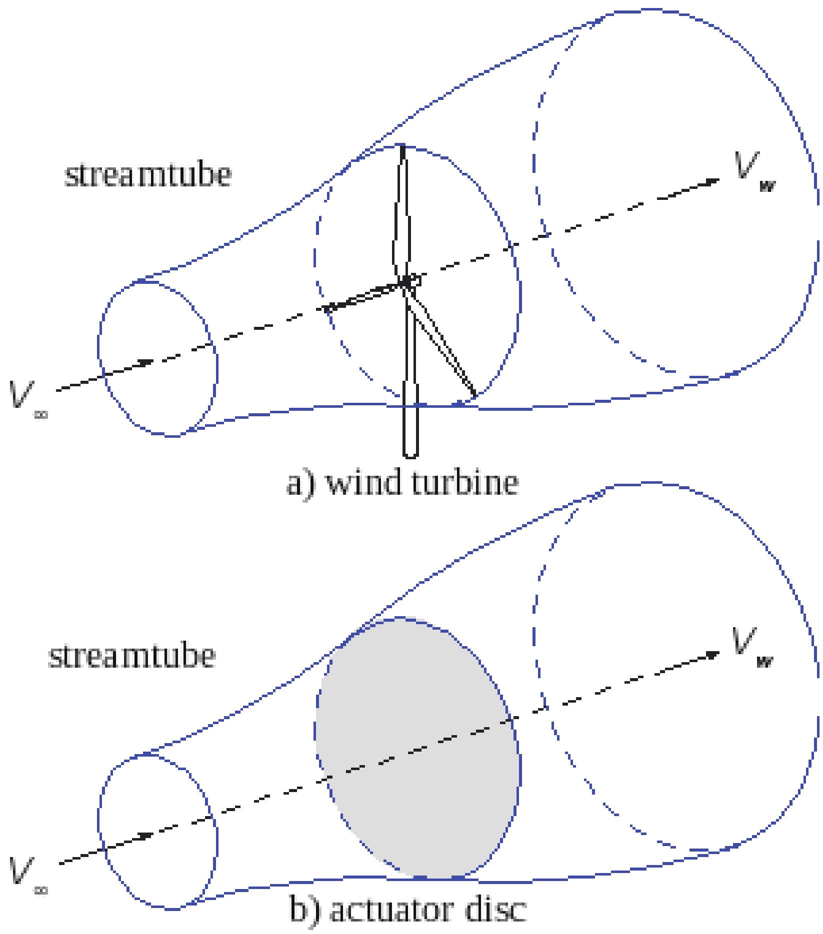

Figure 1: Flowfield of a Wind Turbine and Actuator disc.

Table 1: Properties of the actuator disk.

1.	The flow is perfect fluid, steady, and incompressible.
2.	The actuator disc models the turbine blades and the disc extracts energy from the flow.
3.	The actuator disc creates a pressure discontinuity across the disc.
4.	The flow is uniform through the disc and in the wake.
5.	The disc does not impart any swirl to the flow. The influence of wake rotation will be added later in this chapter.

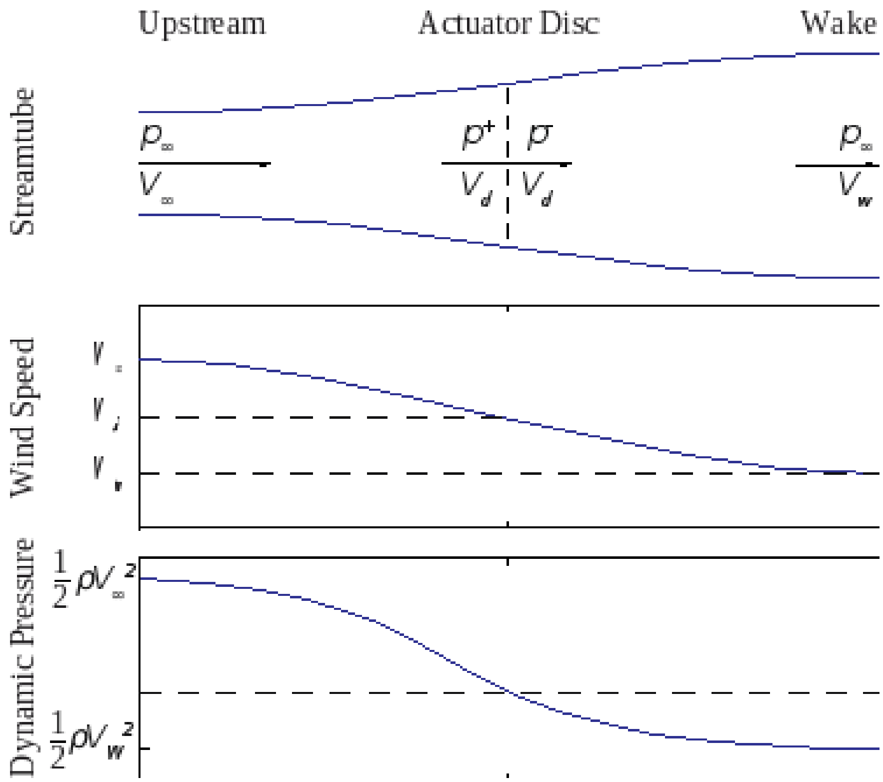

Figure 2: Variation of the velocity and dynamic pressure through the stream-tube.

$$(\rho AV)_\infty = (\rho AV)_d = (\rho AV)_w \tag{1}$$

$$(AV)_\infty = (AV)_d = (AV)_w \tag{2}$$

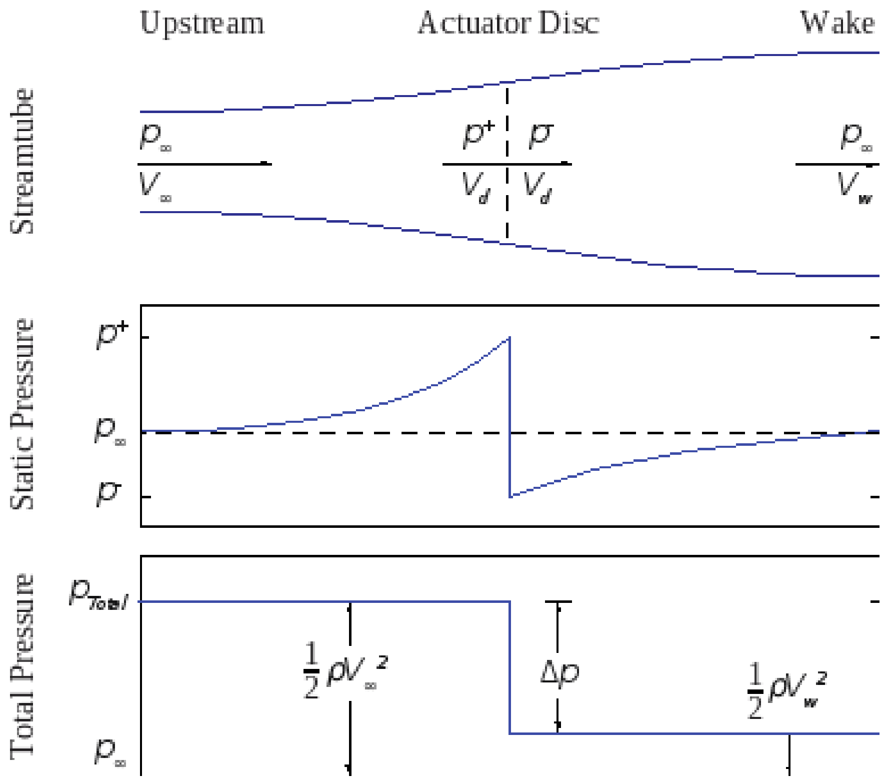

Figure 3: Variation of the static and total pressure along the steam-tube.

$$p_\infty + \frac{1}{2}\rho V_\infty^2 = p^+ + \frac{1}{2}\rho V_d^2 \tag{3}$$

$$p^- + \frac{1}{2}\rho V_d^2 = p_\infty + \frac{1}{2}\rho V_w^2 \tag{4}$$

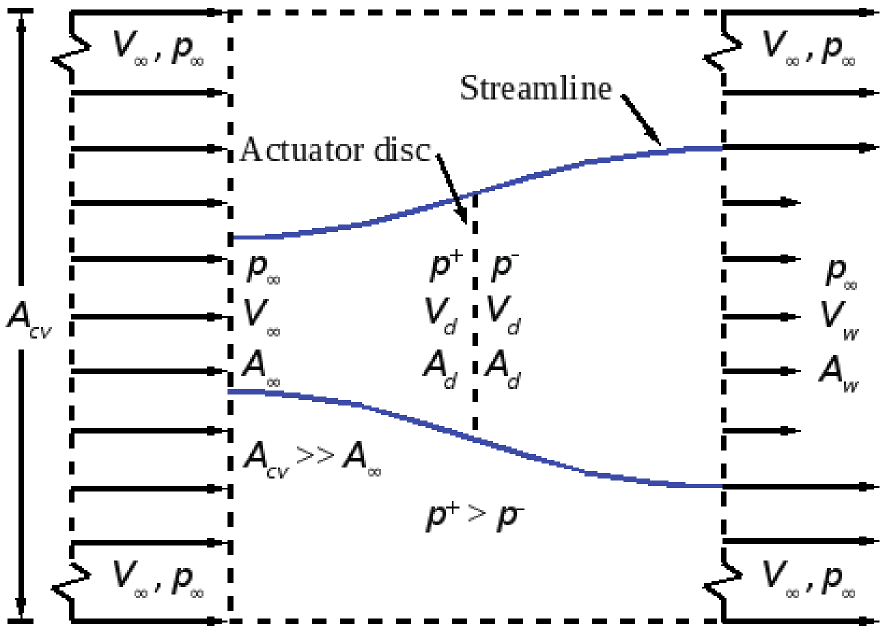

Figure 4: Cylindrical Control Volume surrounding the stream-tube.

$$\sum F_x = -T = \rho V_w^2 A_w + \rho V_\infty^2 \left[A_{cv} - A_w\right] + \dot{m}_{side} V_\infty - \rho V_\infty^2 A_{cv} \tag{5}$$

$$\dot{m}_{side} = \rho A_{cv} V_\infty - \rho A_w V_w - \rho \left[A_{cv} - A_w\right] V_\infty \tag{6}$$

or

$$\dot{m}_{side} = \rho A_w \left[V_\infty - V_w\right]. \tag{7}$$

Therefore

$$T = \rho A_w \left[V_\infty V_w - V_w^2\right] = \rho A_w V_w \left[V_\infty - V_w\right] = \rho A_d V_d \left[V_\infty - V_w\right] \tag{8}$$

- The thrust can also be expressed in terms of the pressure drop across the actuator disc times the area of the disc,

$$T = \Delta p A_d. \tag{9}$$

- But

$$\Delta p = \frac{1}{2}\rho\left[V_\infty^2 - V_w^2\right] \tag{10}$$

so that the thrust acting on the actuator disc can then be expressed as

$$T = \frac{1}{2}\rho A_d\left[V_\infty^2 - V_w^2\right]. \tag{11}$$

- A relationship between the velocity at the actuator disc, V_d, the free-stream velocity, V_∞, and the velocity in the wake, V_w, is

$$V_d = \frac{1}{2}\left[V_\infty + V_w\right]. \tag{12}$$

- Thus we introduce a <u>new parameter</u> that measures how much the wind velocity, V_∞ has been affected by the actuator disc, called the **axial induction factor, a,**

$$a = \frac{V_\infty - V_d}{V_\infty} \tag{13}$$

- The velocity at the actuator disc, V_d, can now be expressed in terms a

$$V_d = V_\infty\left[1 - a\right]. \tag{14}$$

- The wake velocity, V_w, can also be expressed in terms a, and V_∞

$$V_w = V_\infty\left[1 - 2a\right]. \tag{15}$$

- The the thrust on the rotor can be expressed in terms of a

$$T = 2\rho A_d V_\infty^2 a\left[1 - a\right] \tag{16}$$

- Defining the thrust coefficient as

$$C_T = T/\left[\frac{1}{2}\rho A_d V_\infty^2\right] \tag{17}$$

  then

$$C_T = 4a\left[1 - a\right]. \tag{18}$$

- The power extracted from the wind by the actuator disc is equal to the product of the thrust, T, and the wind velocity at the actuator disc, V_d,

$$P = TV_d. \tag{19}$$

- Therefore

$$P = 2\rho A_d V_\infty^3 a \left[1 - a\right]^2 . \tag{20}$$

- The power coefficient, C_p, is defined as the ratio of the power extracted from the wind, P, and the available power of wind, or

$$C_P = P / \left[\frac{1}{2}\rho A_d V_\infty^3\right] \tag{21}$$

- In terms of a,

$$C_P = 4a \left[1 - a\right]^2 . \tag{22}$$

- To find the maximum thrust coefficient, C_T, with respect to a

$$\begin{aligned}\frac{dC_T}{da} &= \frac{d}{da}\left[4a(1-a)\right] \\ &= 4 - 8a \equiv 0 \\ \text{therefore} & \\ a &= 1/2 \\ \text{and} & \\ C_{T_{max}} &= 1\end{aligned} \tag{23}$$

- The maximum power coefficient is obtained similarly

$$\begin{aligned}\frac{dC_P}{da} &= \frac{d}{da}\left[4a(1-a)^2\right] \\ &= 1 - 4a + 3a^2 \equiv 0 \\ \text{therefore} & \\ a &= [1, 1/3] \\ \text{and} & \\ C_{P_{max}} &= \frac{4}{3}\left[1 - \frac{1}{3}\right]^2 \\ &= \frac{16}{27} \\ \text{or,} & \\ C_{P_{max}} &= 0.593\end{aligned} \tag{24}$$

- The maximum theoretical power coefficient, $C_{P_{max}} = 0.593$, is often referred to as the Betz limit after Albert Betz[**?**], who published this finding in 1920.

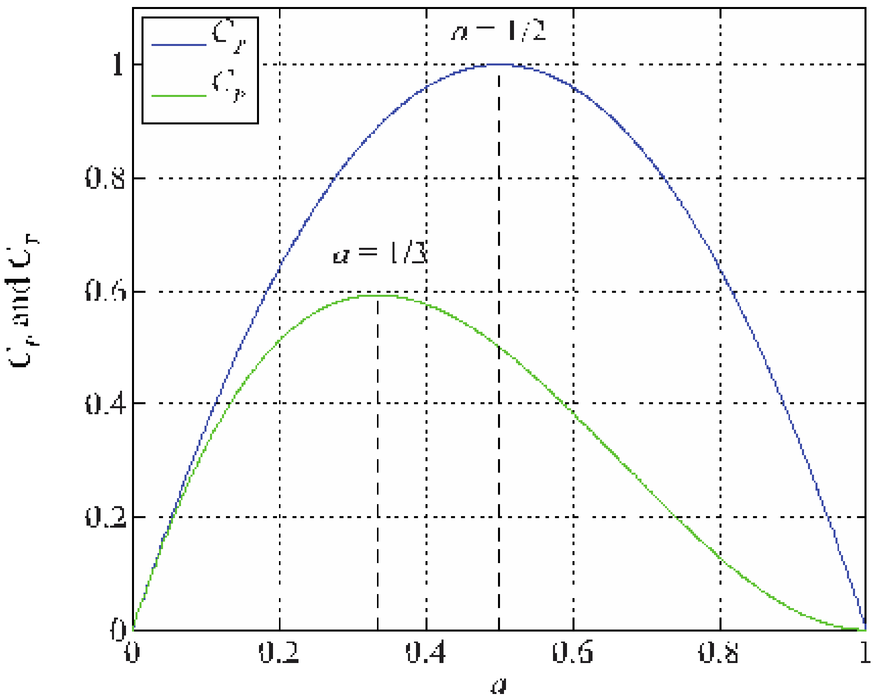

Figure 5: Variation of the rotor thrust and power coefficients, C_T and C_P, with the axial induction factor, a.

Example 1: The following figure shows a stream-tube/actuator disc model of a wind turbine. Assume that the actuator disc has a radius of 3 m. and a freestream wind speed of $V_\infty = 7$ m/s.

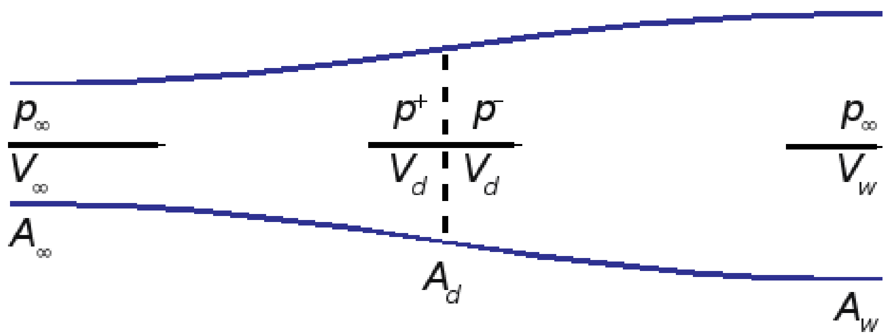

a. Estimate the maximum power that can be extracted by the idealized wind turbine.

b. Determine the velocity at the actuator disc and in the wake.

c. Determine the areas, A_∞ and A_w.

Solution:

a. The power extracted by the actuator disc is give by Eq. 21, and the maximum power coefficient, $C_{P_{max}} = 0.593$, is given by the Betz limit given in Eq 24.

Therefore knowing the actuator disc radius, the disk area is

$$A_d = \pi R^2 = \pi 3^2 = 28.27\text{m}^2.$$

The power extracted by the actuator disc is then

$$C_P = P / \left[\frac{1}{2}\rho A_d V_\infty^3\right]$$

so that

$$P = 0.593(0.5)(1.22\text{kg/m}^3)(7\text{m/s})^3(28.27\text{m}^2) = 3.51\text{kW}.$$

b. The velocity at the actuator disc, V_d, and in the wake, V_w, can be calculated from Eqs. 14 and 15, respectively. Since the power coefficient is a maximum, then $a = 1/3$ so that

$$V_d = V_\infty [1 - a] = 7\text{m/s} \left[1 - \frac{1}{3}\right] = 4.667\text{m/s}$$

and

$$V_w = V_\infty [1 - 2a] = 7\text{m/s} \left[1 - \frac{2}{3}\right] = 2.333\text{m/s}.$$

c. The areas A_∞ and A_w can be calculated using the continuity equation, Eq. 2, namely,

$$(AV)_\infty = (AV)_d = (AV)_w.$$

Therefore,

$$A_\infty = \frac{A_d V_d}{V_\infty} = (28.27\text{m}^2)(4.667\text{m/s})/(7\text{m/s}) = 18.85\text{m}^2$$

and

$$A_w = \frac{A_d V_d}{V_w} = (28.27\text{m}^2)(4.667\text{m/s})/(2.333\text{m/s}) = 56.55\text{m}^2.$$

In this example we see that the velocity of the wind in the wake, V_w, has been reduced to 1/3 of the ambient wind speed, V_∞, and the area of the wake, A_w is three-times as large as that of the stream tube far upstream of the actuator disc, A_∞, or twice the cross-sectional area of actuator disc, A_d.

2 Momentum Theory with Wake Rotation

- The previous momentum theory for the rotor disk provided the optimum inflow induction factor, $a = 0.33$, to maximize the power coefficient, $C_{P_{max}} = 0.593$.
- That analysis assumed that the rotor disk **did not generate any rotation of the flowfield in the wake**
- The following considers the effect of rotation and seeks the conditions that maximize the power coefficient, C_P

Videos:
https://youtu.be/8GVCizBYYUk
https://www.youtube.com/watch?v=L8Ddg6dPwkU

- The momentum analysis is modified to allow the actuator disc to impart rotation to the flow downstream of the disc.
  - The flow upstream of the actuator disc is not affected by the disc rotation.
  - Immediately behind the actuator disc, a tangential flow is imparted to the downstream wake.

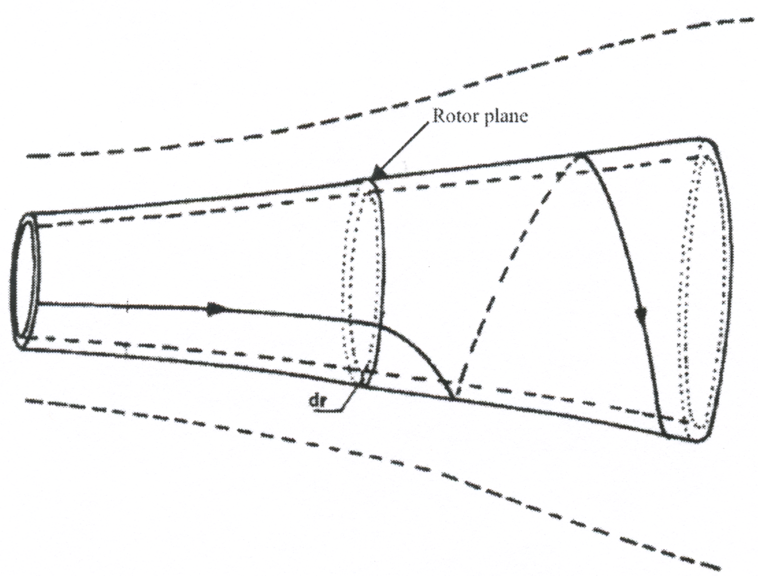

Figure 6: Schematic of the induced rotation of the flow downstream of the rotating actuator disc.

- The tangential flow is represented through an angular induction factor, a', where

$$a' = \frac{\omega}{2\Omega} \tag{25}$$

  - Ω is the angular velocity of the rotor disk
  - ω is the angular velocity imparted to the wake
  - and $\omega \ll \Omega$

- Following Glauert, the differential thrust on an annular ring of the actuator disc is

$$dT \;=\; \Delta p(2\pi r dr) \;=\; \left[\rho\left(\Omega + \frac{\omega}{2}\right)\omega r^2\right] 2\pi r dr \qquad (26)$$

- Introducing a',

$$dT = 4a\,(1+a)\,\frac{1}{2}\rho\Omega^2 r^2\,(2\pi r dr)\,. \qquad (27)$$

- The thrust obtained with *no wake rotation* (Eq. 16), now written in differential form is

$$dT = 2\rho V_\infty^2 a(1-a)(2\pi r dr). \qquad (28)$$

- Equating the two equations for differential thrust, gives that

$$\frac{a(1-a)}{a(1+a)} = \left(\frac{\Omega r}{V_\infty}\right)^2 = \lambda_r^2 \qquad (29)$$

- λ_r is called the local speed ratio, defined as

$$\lambda_r = \frac{\Omega r}{V_\infty}. \qquad (30)$$

- An *important performance parameter for a wind turbine* is the rotor tip-speed-ratio, $\lambda = \lambda_{r=R}$, namely

$$\lambda = \frac{\Omega R}{V_\infty}. \qquad (31)$$

- To determine the *torque* on the rotor, apply conservation of angular momentum
- This yields an equation for the differential torque acting on an angular ring at radius r of the actuator disc

$$dQ \,=\, d\dot{m}\omega r^2 \,=\, \rho V_d\,(2\pi r dr)\,\omega r^2 \tag{32}$$

- Substituting V_d and ω

$$dQ = 2a'(1-a)\rho V_\infty \Omega r^2 (2\pi r dr) \tag{33}$$

- The differential power is

$$dP = \Omega dQ = 2a'(1-a)\rho V_\infty \Omega^2 r^2 (2\pi r dr). \tag{34}$$

- Equating the differential power with wake rotation with that with no wake rotation then

$$\underbrace{2a'(1-a)\rho V_\infty \Omega^2 f^2 (2\pi r dr)}_{with\,rotation} = \underbrace{2a(1-a)^2 \rho V_\infty^3 (2\pi r dr)}_{without\,rotation}. \tag{35}$$

- Simplifying leads to a useful relation

$$a(1-a) = a'\lambda_r^2. \tag{36}$$

- The incremental *power coefficient* for an annular ring is

$$dC_P = \frac{dP}{\frac{1}{2}\rho V_\infty^3} A_d. \tag{37}$$

- Substituting for $dP = \Omega dQ$

$$\begin{aligned} dC_P &= \frac{2a'(1-a)\rho V_\infty \Omega^2 r^2 (2\pi r dr)}{\frac{1}{2}\rho V_\infty^3 \pi R^2} \\ &= \frac{[8a'(1-a)\lambda_r^2 r dr]}{R^2} \end{aligned} \tag{38}$$

- Introducing the variable, μ, where

$$\mu = \frac{r}{R} \tag{39}$$

and

$$d\mu = \frac{dr}{R} \tag{40}$$

- Then dC_P can be integrated with respect to μ to give

$$C_P = 8\int_0^1 a'(-a)\lambda_r^2 \mu d\mu. \tag{41}$$

- Example 2: Determine the conditions on the inflow induction factor, a that maximizes the power coefficient with rotation

$$C_P = 8\int_0^1 a'(-a)\lambda_r^2 \mu d\mu \tag{42}$$

- Solution: Find the condition on a that maximizes the integrand, namely

$$\frac{d}{da}\left[8a'(1-a)\lambda_r^2\mu\right] = 0 \tag{43}$$

or

$$8\lambda_r^2\mu\left[1 - a - a'\frac{da}{da'}\right] = 0 \tag{44}$$

which yields

$$\frac{da}{da'} = \frac{1-a}{a'} \tag{45}$$

- From before,

$$a(1-a) = a'\lambda_r^2 \tag{46}$$

- Taking d/da', then

$$\frac{da}{da'} = \frac{\lambda_r^2}{1-2a} \tag{47}$$

- Equating the two expressions for d/da' gives

$$\frac{1-a}{a'} = \frac{\lambda_r^2}{1-2a} \tag{48}$$

or

$$\lambda_r^2 a' = (1-a)(1-2a) \tag{49}$$

- Substituting

$$\lambda_r^2 a' = a(1-a) \tag{50}$$

then

$$a(1-a) = (1-a)(1-2a) \tag{51}$$

- Solving for a we obtain

$$a = 1/3 \tag{52}$$

- **Thus** $a = 1/3$ **gives** $C_{P_{max}}$ **without and rotation**.

- Substituting $a = 1/3$ gives

$$a' = \frac{a(1-a)}{\lambda_r^2} = \frac{2/9}{\lambda_r^2} \tag{53}$$

- Thus a' decreases with increasing r on the rotor
  - Therefore wake rotation is a minimum at the rotor tip, and a maximum at the rotor root.

3 Blade Element Momentum (BEM) Theory

- Actuator disc theory provides us with simple formulas to calculate the power extracted and thrust acting on the wind turbine rotor.
- It provided a theoretical limit on the power that can be extracted from the wind.
- However it is unable to predict the performance of wind turbine rotor blades as a function of the *rotor blade design parameters* such as
  1. rotor radius,
  2. number of blades,
  3. blade chord,
  4. blade twist,
  5. airfoil section shape,
  6. and radial variations of these.
- Ihe objective is to optimize the aerodynamic performance and thereby maximize the power output of the wind turbine.

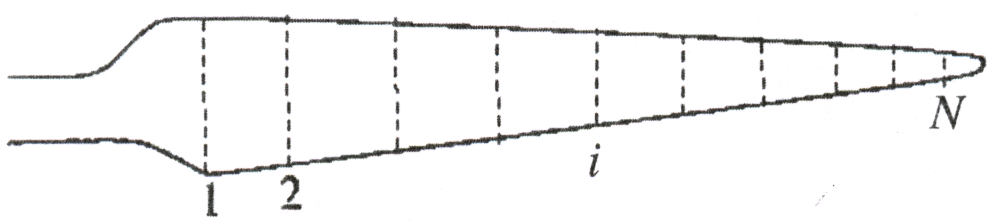

Figure 7: Example of a wind turbine blade divided into 10 sections for BEM analysis.

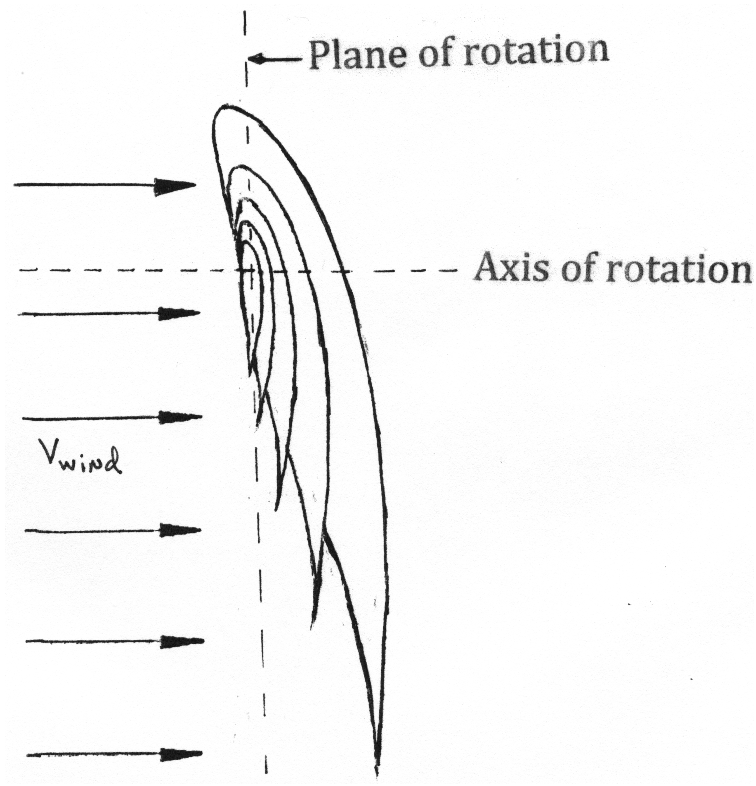

Figure 8: Example of the variation in chord and geometric twist along the radial distance of a wind turbine rotor blade.

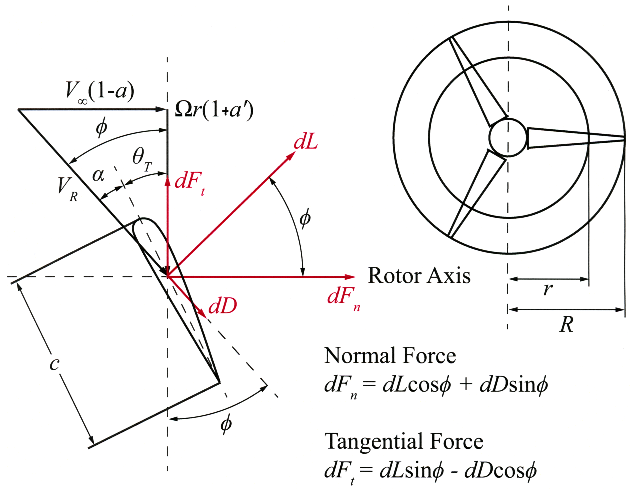

Figure 9: Illustration of the aerodynamic forces acting on a wind turbine blade section at a distance r from the axis of rotation.

- The angle of attack of the airfoil section on the rotor is the angle between the airfoil chord line and the resultant velocity the airfoil section experiences
- With rotation, the resultant velocity, V_R, is made up of the vector sum of the wind speed and the rotational speed of the blade section
$$V_R = \sqrt{[V_\infty(1-a)]^2 + [\Omega r(1+a')]^2} \tag{54}$$
- Note that both the wind speed and rotation velocities are modified by the axial and angular induction factors

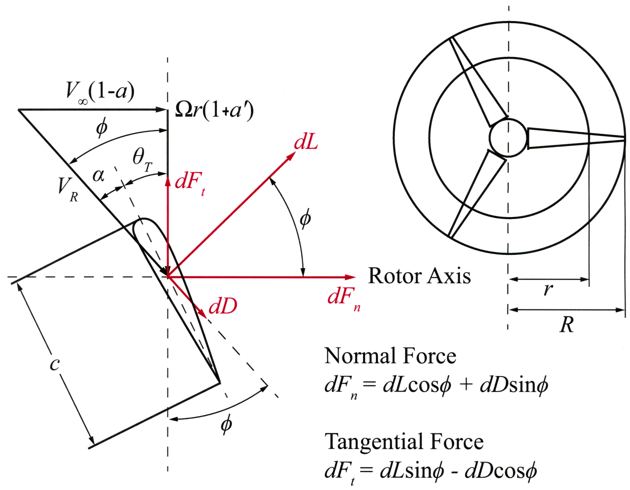

Figure 10: Illustration of the aerodynamic forces acting on a wind turbine blade section at a distance r from the axis of rotation.

- The angle that the resultant velocity makes with respect to the plane of rotation is the angle, ϕ, where

$$\tan\phi = V_\infty \frac{1-a}{\Omega r(1+a')} \tag{55}$$

so that

$$\phi = \tan^{-1}\left[\frac{V_\infty(1-a)}{\Omega r(1+a')}\right]. \tag{56}$$

- Wind turbine blade must have a built-in twist distribution from the hub to the tip, so that each blade section will be at an angle of attack that is near that of $(L/D)_{max}$.
- The blade can be also mounted into the hub at some desired *pitch angle*, θ_{cp}.
  - It is usually measured as angle relative to the plane of rotation
  - For a fixed pitch blade, θ_{cp} is a constant
  - In a pitch controlled wind turbine, θ_{cp}, is varied to control the power output between rated and cut-out wind speeds.
- The local angle of attack, α, at any radial location on the rotor is the sum of the local resultant velocity vector angle, $\phi(r)$, minus the local twist angle, $\theta_T(r)$, and the pitch angle, θ_{cp}, namely

$$\alpha(r) = \phi(r) - [\theta_T(r) + \theta_{cp}] . \tag{57}$$

- The **thrust** force acting on any section of the rotor blade section acts normal to the plane of rotation of the blade.
- The **torque** on any section of the blade equals the net aerodynamic force in the plane of rotation times its distance to the axis of rotation
- The normal and tangential forces on a section of the blade can be expressed in terms of the **differential** lift and drag forces

$$dL = C_L \frac{1}{2} \rho V_R^2 c dr \tag{58}$$

and

$$dD = C_D \frac{1}{2} \rho V_R^2 c dr \tag{59}$$

- The lift and drag coefficients are functions of the airfoil section angle of attack, α.
- The differential force normal to the plane of rotation, dF_n, and the differential tangential force in the plane of rotation, dF_t are

$$dF_n = dL \cos\phi + dD \sin\phi \tag{60}$$

and

$$dF_t = dL \sin\phi - dD \cos\phi \tag{61}$$

- Substituting for dL and dD and letting B represent the number of blades, the differential normal and tangential forces are

$$dF_n = B \frac{1}{2} \rho V_R^2 \left[C_L \cos\phi + C_D \sin\phi \right] c dr \tag{62}$$

and

$$dF_t = B \frac{1}{2} \rho V_R^2 \left[C_L \sin\phi - C_D \cos\phi \right] c dr. \tag{63}$$

- Defining

$$C_n = C_L \cos\phi + C_D \sin\phi \tag{64}$$

and

$$C_t = C_L \sin\phi - C_D \cos\phi \tag{65}$$

- Then

$$dF_n = B\frac{1}{2}\rho V_R^2 C_n c dr \tag{66}$$

and

$$dF_t = B\frac{1}{2}\rho V_R^2 C_t c dr. \tag{67}$$

- The differential torque, $dQ = rdF_t$ and the differential power, $dP = \Omega dQ$ are then

$$dQ \;=\; rdF_t \;=\; B\frac{1}{2}\rho V_R^2 C_t crdr \tag{68}$$

and

$$dP \;=\; \Omega dQ \;=\; B\Omega\frac{1}{2}\rho V_R^2 C_t crdr. \tag{69}$$

- To incorporate a and a', the thrust determined by momentum theory with no wake rotation is used, namely

$$dT = 2\rho V_\infty^2 a(1-a)2\pi rdr. \tag{70}$$

- The differential thrust, dT, is equivalent to the differential normal force, dF_n. Therefore equating these

$$\underbrace{2\rho V_\infty^2 a(1-a)2\pi rdr}_{Momentum\,Theory} = \underbrace{B\frac{1}{2}\rho V_R^2 C_n cdr}_{BEM\,Theory}. \tag{71}$$

- Substituting

$$V_R = \frac{V_\infty(1-a)}{\sin\phi}. \tag{72}$$

and rearranging terms

$$\frac{a}{1-a} = \frac{BC_n c}{8\pi r\sin^2\phi}. \tag{73}$$

- Defining a new parameter, σ_r where

$$\sigma_r = \frac{Bc}{2\pi r} \tag{74}$$

then

$$a = \frac{1}{\frac{4\sin^2\phi}{\sigma_r C_n} + 1}. \tag{75}$$

- Similarly equating the torque equations from momentum amd BEM theories

$$\underbrace{2a'(1-a)\rho V_\infty \Omega r^2 2\pi r dr}_{Momentum\,Theory} = \underbrace{B\Omega\frac{1}{2}\rho V_R^2 C_t c r dr}_{BEM\,Theory} \tag{76}$$

one obtains a relation for the angular induction factor

$$a' = \frac{1}{\frac{4\sin\phi\cos\phi}{\sigma_r C_t} - 1}. \tag{77}$$

- We will discuss how the BEM equations are solved for a wind turbine design a little later.

4 Prandtl's Tip Loss Factor

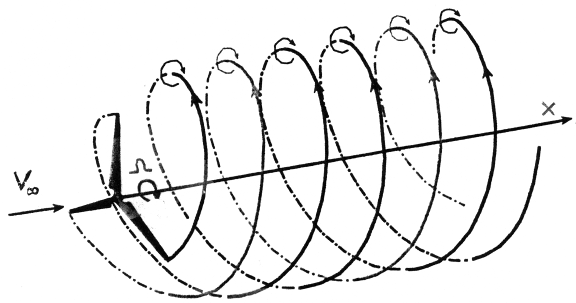

Figure 11: Illustration of rotor tip vortices from a three-bladed wind turbine rotor.

Figure 12: Photograph of the cross-section of the tip vortices from a two-bladed wind turbine that was visualized in a wind tunnel experiment[?].

- The vortices that form at the tip of the rotor result in added drag that was not accounted for in the momentum analysis.
- The BEM approach assumes that each section of the rotor is independent of the neighbor sections.
  - This is a reasonable assumption for the inboard portion of the rotor blade
  - However significant interference occurs on the outboard radial portion of the rotor blades
  - Specifically at the rotor tip, flow from the high pressure side of the rotor blade passes around the blade tip to the lower pressure side
  - Observed as a “tip vortex”

- The effect of the tip vortices is to lower the lift and therby the generated torque, at the outboard portion of the blade.
- Ludwig Prandtl developed a *tip loss factor*, F,

$$F = \frac{2}{\pi} \cos^{-1}\left(e^{-f}\right) \tag{78}$$

where

$$f = \frac{B}{2} \frac{R - r}{r \sin \phi} \tag{79}$$

  - B is the number of rotor blades,
  - r is the local radius on the rotor,
  - R is the rotor radius,
  - ϕ is the local angle the resultant velocity makes with the rotor disk plane of rotation at the local radius.
- The tip loss factor is introduced into the differential thrust such that

$$dT = 2F\rho V_\infty^2 a(1 - a)2\pi r dr. \tag{80}$$

and

$$dQ = 2Fa'(1 - a)\rho V_\infty \Omega r^2 (2\pi r dr). \tag{81}$$

- The differential torque relates to the differential power as

$$dP = \Omega dQ. \tag{82}$$

- Generally

$$r/R \leq 0.6: \;\; F \simeq 1 \tag{83}$$

$$r/R > 0.6: \;\; F < 1 \tag{84}$$

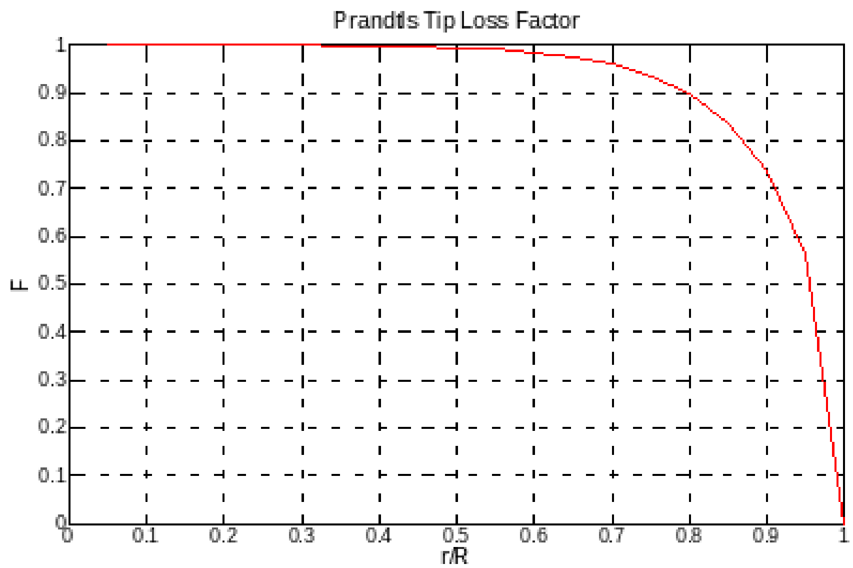

Figure 13: Prandtl tip loss factor along the span of a wind turbine rotor.

- Equating the differential momentum equation for thrust and torque including the Prandtl tip loss factor, with the corresponding differential thrust and torque equations

$$a = \frac{1}{\frac{4F\sin^2\phi}{\sigma_r C_n} + 1} \quad (85)$$

and

$$a' = \frac{1}{\frac{4F\sin\phi\cos\phi}{\sigma_r C_t} - 1} \quad (86)$$

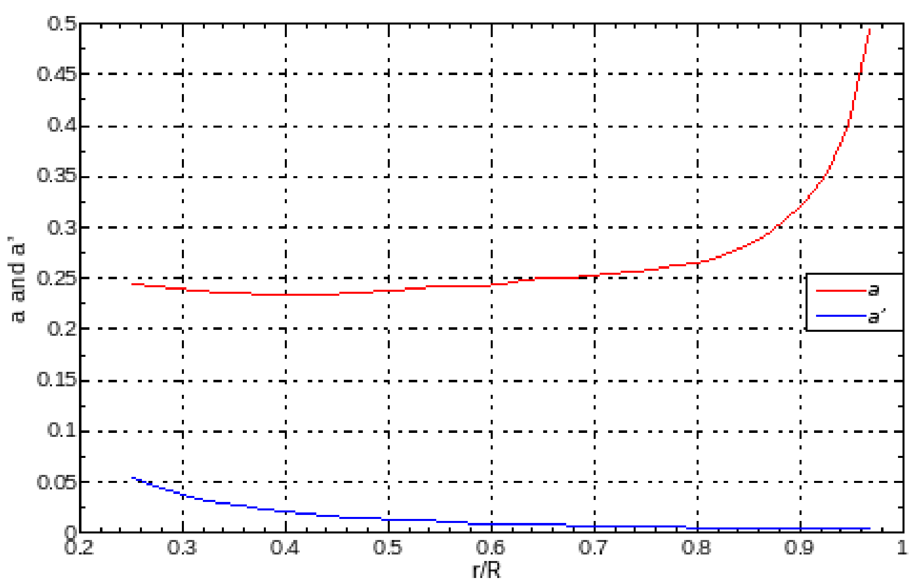

Figure 14: Spanwise distribution of the induction factors, a and a' for the University of Notre Dame Research Wind Turbines.

5 Solution of the BEM Equations

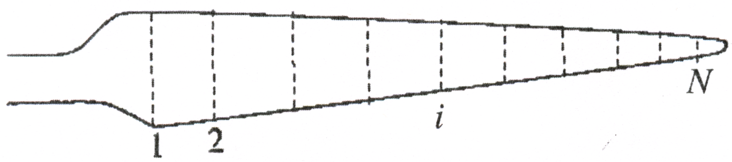

Figure 15: Example of a wind turbine blade divided into 10 sections for BEM analysis.

- For a given tip speed ratio, λ, and a wind speed, V_∞, an iterative approach can be used to determine the axial and rotational induction factors a and a', at a given station on the blade.
- Once the induction factors are known, the differential thrust, torque and power at that station can be determined.
- This process is continued for each segment across the blade.
- The differential components of thrust, torque and power can then be summed to obtain the total thrust transmitted to the tower and the total torque and power delivered to the drive shaft. A flow chart that illustrates this approach is shown in Figure 16.

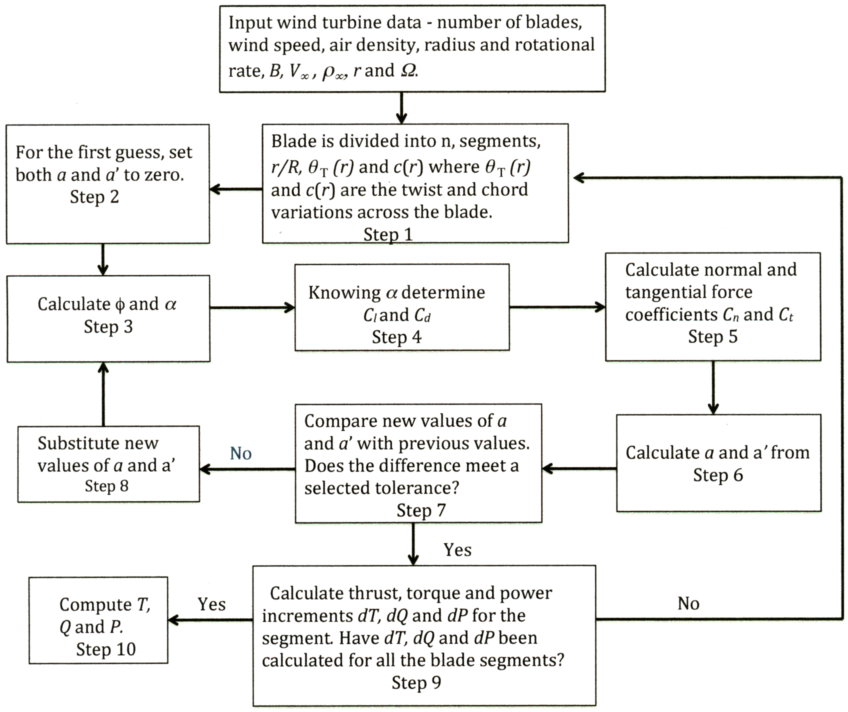

Figure 16: Flow Chart for the iterative procedure used in solving the BEM equations.

Step 1.	Divide the blade into n, spanwise segments and input the geometric blade information for each segment.
Step 2.	Start at the most inboard segment.
Step 3.	Set the axial and tangential induction factors, a and a' to zero.
Step 4.	Compute the angles ϕ and α using Eqs. 56 and 57.
Step 5.	Knowing the angle of attack, α, the lift and drag coefficients, C_L and C_D, can be computed from polynomial expressions that are a fit to the lift and drag coefficient data for the airfoil section shape at the given spanwise segment of the rotor.
Step 6.	Calculate the normal and tangential force coefficients, C_n and C_t, from Eqs. 64 and 65.
Step 7.	Calculate a and a' from Eqs. 75, 78, 79, 85 and 86.
Step 8.	Compare the new values of a and a' with the previous values. Does the difference meet the convergence criteria? If "No" go to Step 9 using the new values of a and a'. If "Yes" go to Step 10.
Step 9.	Use the values of a and a' from Step 7 and go to Step 4.
Step 10.	Calculate the differential thrust, dT, torque, dQ, and power, dP, for the blade segment using Eqs. 80 to 82. If this is the last (most outboard) blade segments go to Step 11. Otherwise move to the next blade segment and repeat the process starting at Step 3.
Step 11.	Calculate the total thrust T, torque, Q, and power, P as the sum of the differential power from each of the spanwise segments.

5.1 Example BEM Equation Solution

Figure 17: Photograph of the University of Notre Dame Research Wind Turbines and Meteorological tower.

- The combined efficiency of the power train components, bearings, gearbox, generator, etc. was assumed to be $\eta = 0.9$.
  - That is 90% of the power extracted by the rotor is converted to electrical power.

Table 2: Characteristics of the University of Notre Dame Wind Turbines

Re_c	0.5×10^6
$C_L(\alpha)$	$0.327 + 0.1059\alpha - 0.0013\alpha^2$
$C_D(\alpha)$	$0.006458 - 0.000272\alpha + 0.000219\alpha^2 - 0.0000003\alpha^3$
α	$-2° \leq \alpha 12°$
B	3
λ	7
R	4.953 m.
V_{cut-in}	3.0 m/s
V_{rated}	11.6 m/s
$V_{cut-out}$	37.0 m/s
Rated Power	25 kW

Table 3: Rotor Geometry of the University of Notre Dame Wind Turbines

r/R	Chord (mm)	Blade Twist (°)
0.2414	467.62	14.39
0.2835	421.45	11.89
0.3257	382.21	9.92
0.3678	349.07	8.34
0.4100	323.59	7.05
0.4521	303.19	5.98
0.4943	287.05	5.08
0.5364	274.53	4.31
0.5785	259.42	3.64
0.6207	249.51	3.07
0.6628	239.74	2.56
0.7050	230.16	2.11
0.7471	220.04	1.71
0.7893	211.77	1.34
0.8314	204.56	1.03
0.8736	200.88	0.73
0.9157	196.84	0.47
0.9579	192.37	0.22
1.0000	188.02	0

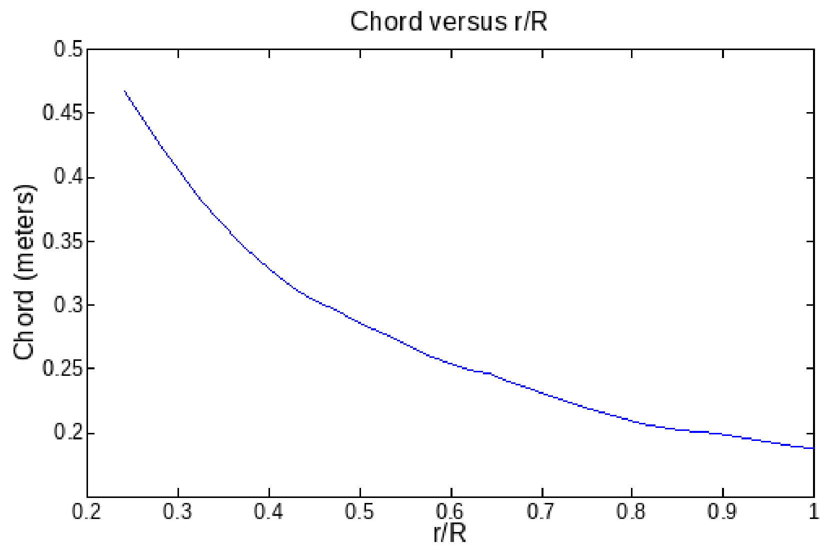

Figure 18: Blade chord distribution for the University of Notre Dame Research Wind Turbines.

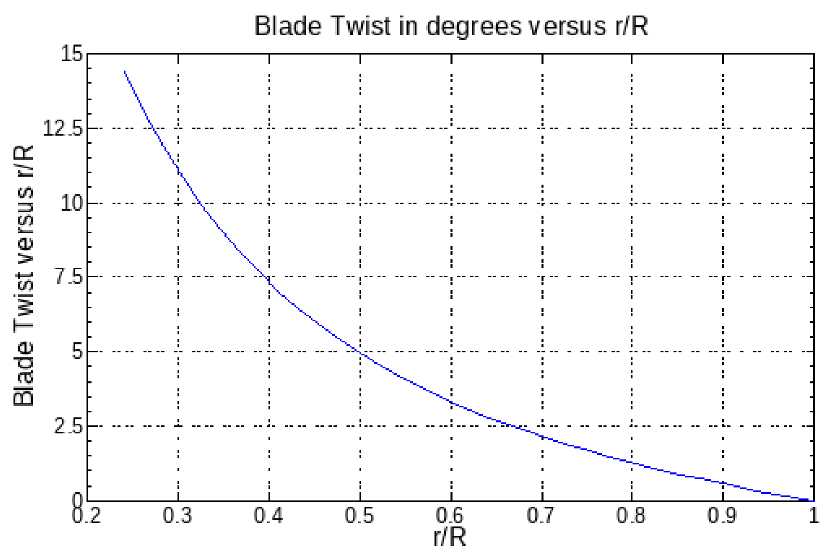

Figure 19: Blade twist distribution for the University of Notre Dame Research Wind Turbines.

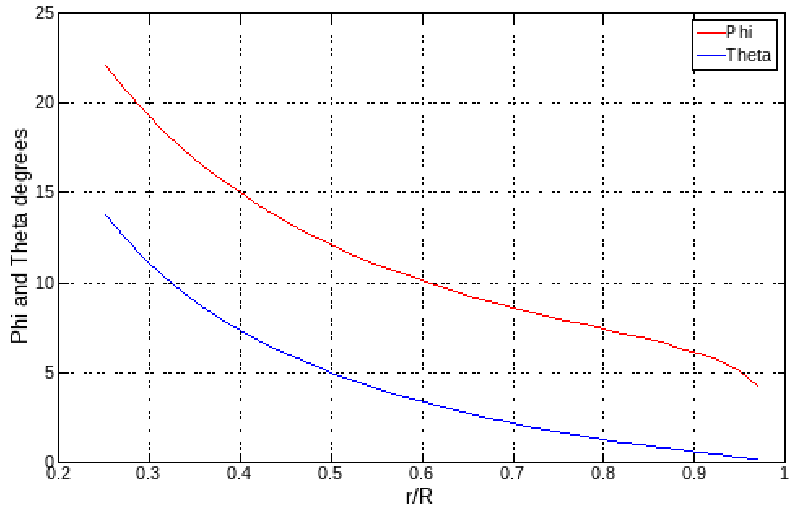

Figure 20: Spanwise distribution of the rotor blade angles ϕ and θ_T for the University of Notre Dame Research Wind Turbines.

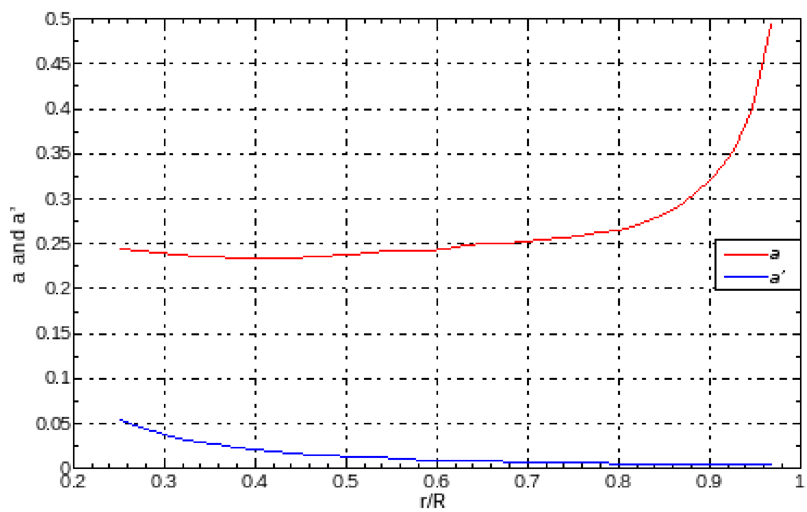

Figure 21: Spanwise distribution of the induction factors, a and a' for the University of Notre Dame Research Wind Turbines.

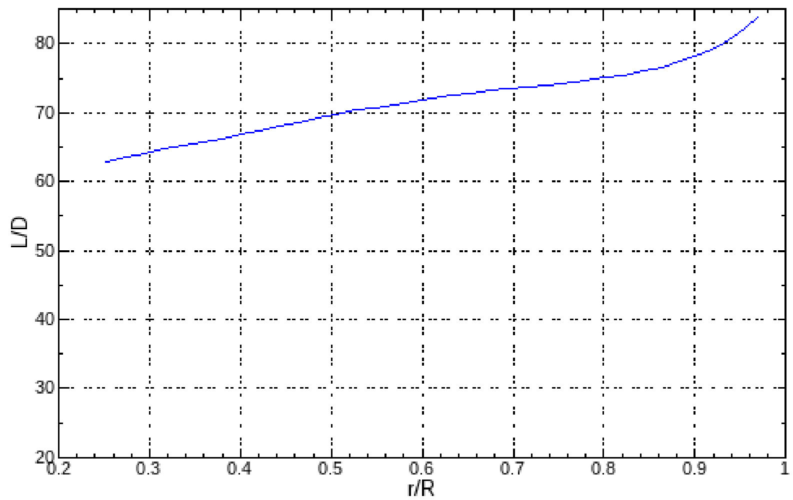

Figure 22: Spanwise distribution of the lift-to-drag ratio for the University of Notre Dame Research Wind Turbines.

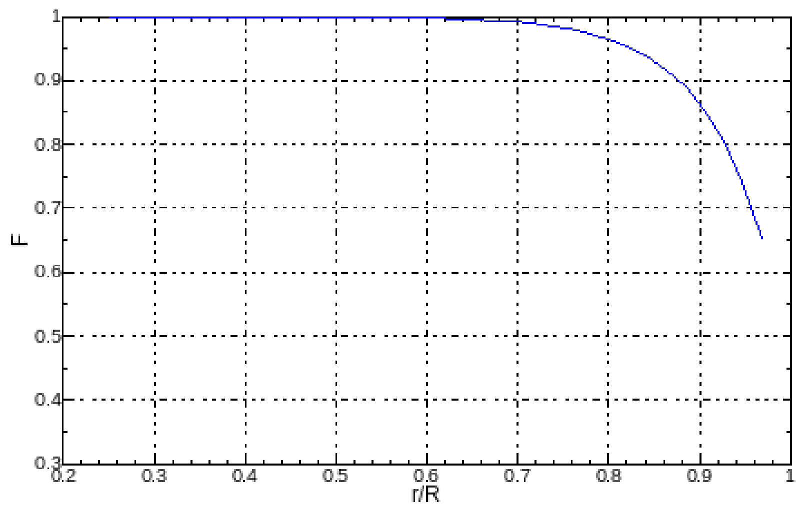

Figure 23: Spanwise distribution of the Prandtl loss coefficient for the University of Notre Dame Research Wind Turbines.

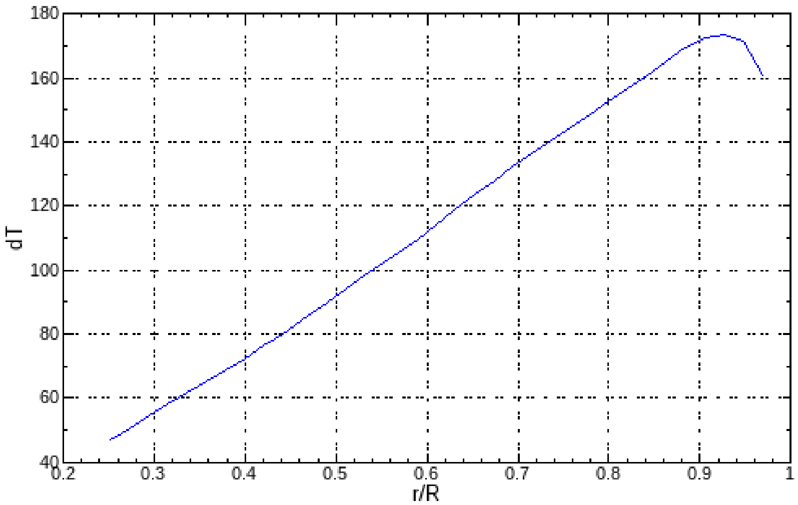

Figure 24: Spanwise distribution of the differential thrust for the University of Notre Dame Research Wind Turbines.

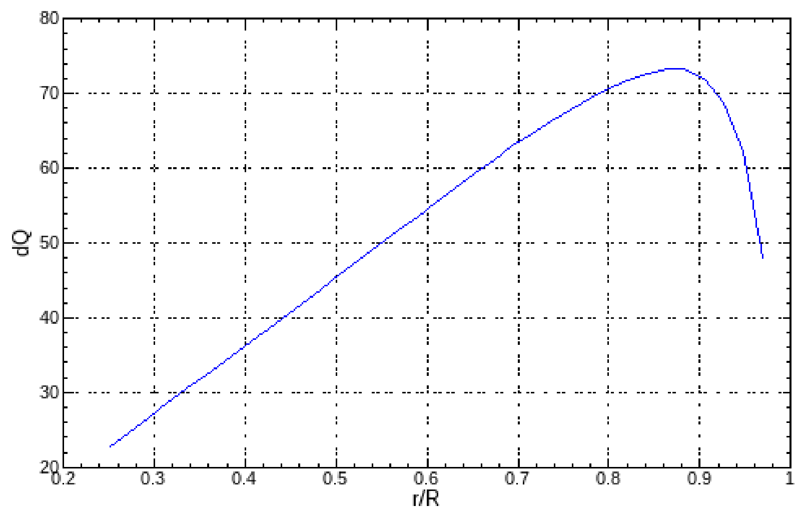

Figure 25: Spanwise distribution of the differential torque for the University of Notre Dame Research Wind Turbines.

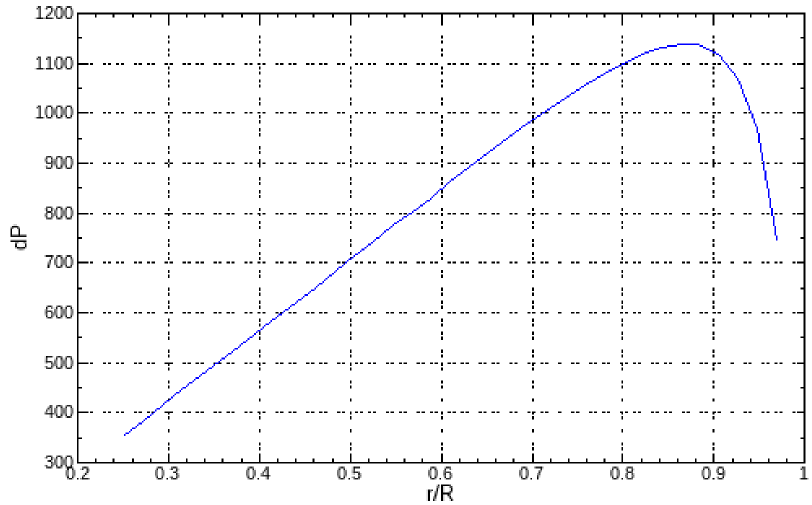

Figure 26: Spanwise distribution of the differential power for the University of Notre Dame Research Wind Turbines.

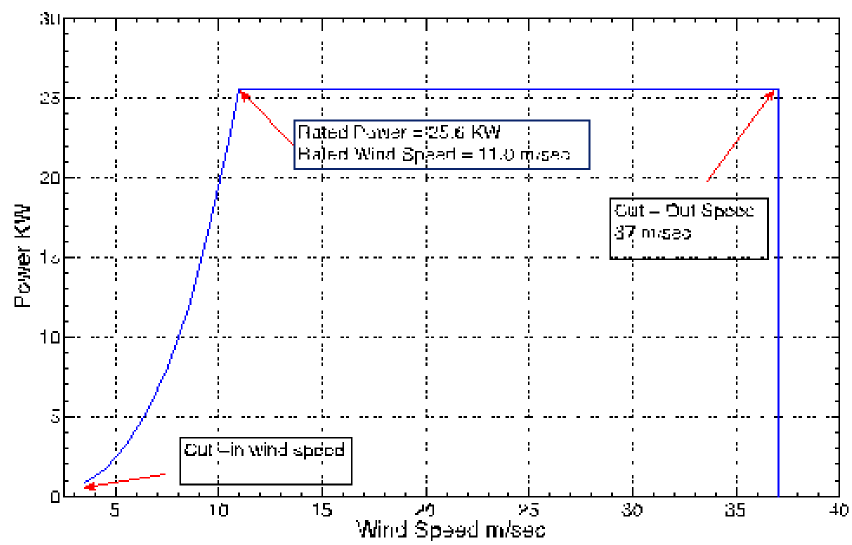

Figure 27: Power curve for the University of Notre Dame Research Wind Turbines.